# ULTRASONIC CHARACTERIZATION OF A THIN LAYER OF ANODIZED POROUS ALUMINUM OXIDE

W. Wang and S.I. Rokhlin

Department of Welding Engineering
The Ohio State University
190 W. 19th Avenue
Columbus, OH 43210

## INTRODUCTION

Formation by anodization of a thin porous layer of aluminum oxide ($Al_2O_3$) on an aluminum surface prior to bonding is required for adhesive joining of aluminum alloys [1,2]. The properties of this layer have major importance for joint strength [1,2].

It is known that aluminum oxide formed by phosphorus anodization has vertical through-thickness pores which form a honeycomb structure. Because of the structure of its pores the oxide layer is elastically anisotropic with one isotropic plane which is parallel to the substrate. The elastic properties of the anodized layer are important for the development of a physical model of the adhesive joint interphase for use in the theoretical simulation of the ultrasonic evaluation of adhesive joints [3].

In this work, the elastic properties of a thin (50 μm) porous anisotropic $Al_2O_3$ layer have been measured by an angle beam transmission technique. The elastic properties have been determined by studying the angle dependence of the transmission minimum and maximum. While measurement of the transmission maxima (reflection minima) for evaluation of composite materials has been widely used previously [4], experimental study of the transmission minima is explored here for the first time. It is shown that coincidence of the angular positions of the transmission minimum and maximum depends in different ways on the in-plane shear and Young's moduli which helps to separate their effects and to measure them simply. The full advantage of transmission minima measurements for reconstruction of elastic properties of composite materials is demonstrated in another paper in this proceeding [5].

The aim of this paper is to reconstruct from experimental data the effective elastic constants of the thin porous oxide layer and by comparing experimental data with different theoretical models to select an appropriate one for this structure. This selection is important for the interphase modeling.

*Review of Progress in Quantitative Nondestructive Evaluation*, Vol. 9
Edited by D.O. Thompson and D.E. Chimenti
Plenum Press, New York, 1990

## THEORY

A theoretical study of ultrasonic interaction with a fluid-coupled orthotropic plate of arbitrary orientation has been published recently by Chimenti and Nayfeh [6]. In this work we are interested in a simplified special case when the incident plane of the ultrasonic wave lies in the plane of symmetry of the anisotropic plate. A matrix method for an anisotropic multilayered structure (each layer of this structure is in a plane of symmetry) has been developed by Solyanik [7] and closed-form solutions for single layers have been given by Nayfeh and Chimenti [4]. A discussion of approximate plate theory for this case has been given by Shenderov [8]. In this paper and accompanying work [3] we implement the matrix algorithm [7] for our calculations.

Figure 1 shows the theoretical transmission coefficient as a function of incident angle which varies in correspondence with variation of the elastic moduli and the product of wave frequency and sample thickness. Figure 1(a) shows the effect of the in-plane Young's modulus, $E_1$. The increase of the in-plane Young's modulus significantly decreases both the angle of transmission minimum and the angle of transmission maximum. Figure 1(b) shows the effect of interlayer shear modulus, $G_{13}$ (subscript 3 denotes the plate normal direction). In contrast to $E_1$, $G_{13}$ affects only the angle of the maximum transmission coefficient, which decreases with the increase of $G_{13}$. Similar calculations have also been made on the other independent elastic constants but no apparent effects were found since the thickness of the plate was much less than the wavelength. Figure 1(c) shows the effect of wave frequency and sample thickness. The angle of maximum transmission coefficient decreases with the increase of the product of frequency and thickness but the angle of minimum transmission coefficient is not affected. This indicates some advantages of the transmission minimum measurement when plate thickness is not precisely known. Additional calculation of the transmission coefficients at different sample densities has also been made and the results shows that both the angles of transmission minimum and of transmission maximum can be significantly affected by sample density. It is apparent from these results that by measuring the sample density and thickness independently, we can restrict the set of variables to the elastic constants, especially $E_1$ and $G_{13}$. Thereafter, we can determine $E_1$ through measurements of the angle of minimum transmission coefficient, and by subsequent optimization to fit the maximum-transmission angle we can reconstruct $G_{13}$.

## EXPERIMENTAL PROCEDURE

The experimental apparatus which implements a novel type of ultrasonic goniometer is shown in Fig. 2. The $Al_2O_3$ sample was mounted in the center of the cylinder and rotated around the cylinder axis which lies in the frontal plane of the sample. The ultrasonic signal transmitted through the sample is reflected from the plane reflector and returned to the transducer after the second through-transmission. The received signal are digitized and averaged by a LeCroy 9400 125 MHz digital oscilloscope and collected by a computer as a function of the angle of rotation. For sample rotation around the cylinder axis a computer controlled DC motor is used. Angle resolution and repeatibility of 0.01° are achieved in our setup.

The water tank is temperature stabilized at 29.8 ± 0.1°C. Thin anodized porous $Al_2O_3$ samples were immersed in the water at least 30 minutes before measurements were conducted to allow complete water penetration into the pores.

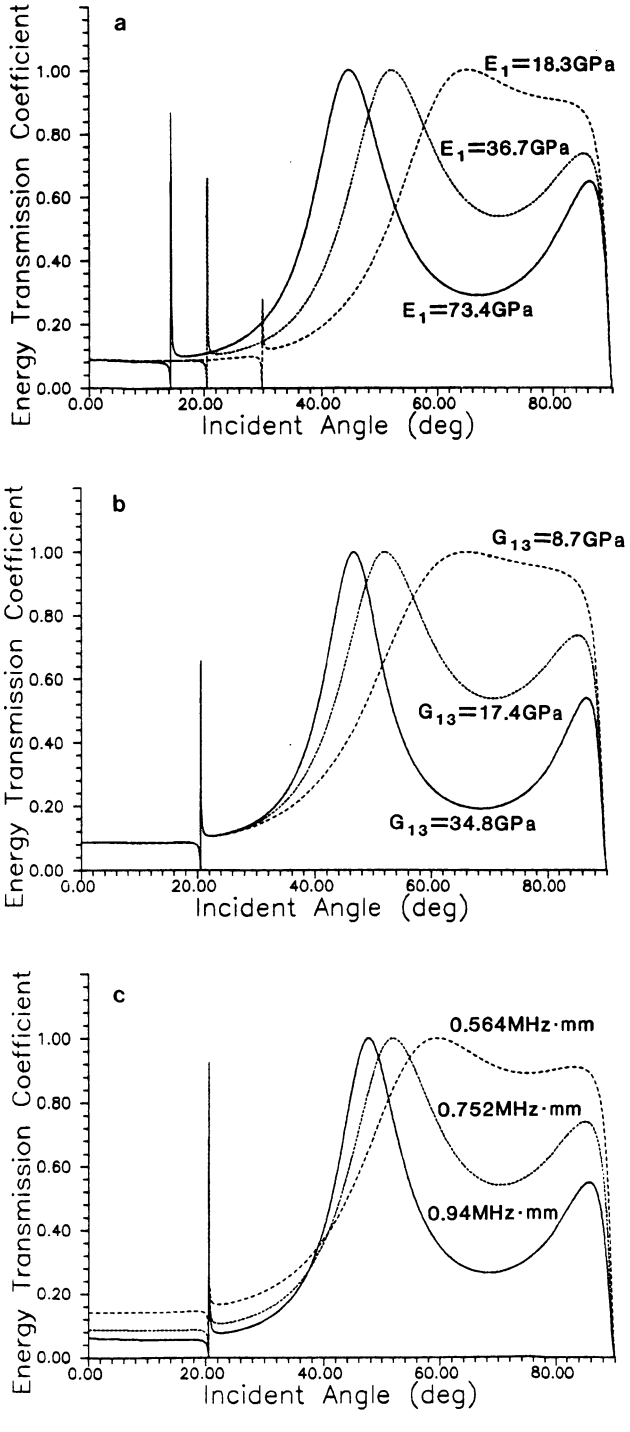


Fig. 1. Dependence of transmission coefficients on elastic constants and and the product of frequency and sample thickness. (a) Effect of in-plane Young's modulus, $E_1$. (b) Effect of interlayer shear modulus, $G_{13}$. (c) Effect of frequency and sample thickness.

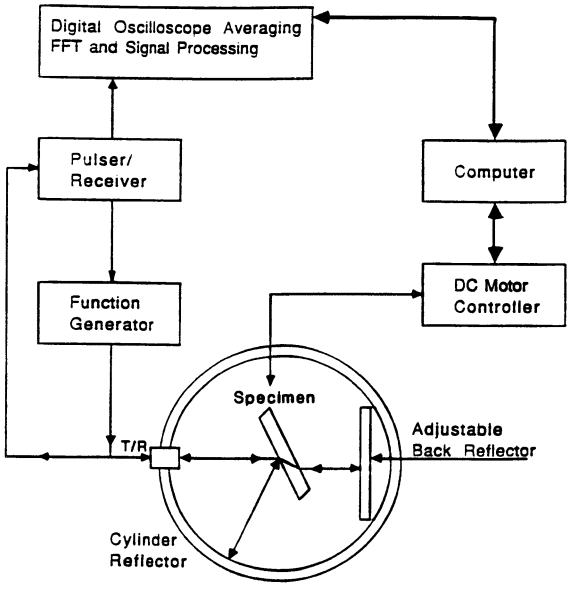


Fig. 2. Configuration of the experimental system.

The surface and cross section of a representative anodized porous $Al_2O_3$ microstructure are shown in Fig. 3. As shown, the thin layer of anodized $Al_2O_3$ contains vertical through-thickness pores, which are discrete and basically uniform in size. The average pore diameter measured from the photomicrograph is about 2000 Å.

Two different methods were utilized to measure the volume fraction of the pores from photomicrographs. One was by cutting the top-view pictures, such as Fig. 3(a), and measuring the weight fraction of the pore area in the picture as the volume fraction of pores in the real structure. The other method was digitizing the top-view pictures into a computer and taking the probability of finding a randomly located spot in the pore area as the volume fraction of pores. The results of both measurements show that the average volume fraction of pores is about 61%.

The sample density was then calculated from the pore volume fraction. For a water-filled $Al_2O_3$ sample with 0.61 pore volume fraction the effective density including liquid was 2.16 g/cm$^3$ (i.e., the density of bulk $Al_2O_3$ is 3.986 g/cm$^3$).

Sample thickness was measured both by a micrometer and from SEM photomicrographs. The result of both measurements is 47 μm.

## COMPARISON OF DENSITY MEASUREMENT RESULTS WITH NORMAL-INCIDENT-TRANSMISSION-COEFFICIENT MEASUREMENT DATA

To check the validity of the calculated density, we can compare the normally-incident transmission coefficients measured from experiment and those calculated from the theory based on the density obtained above. Such a comparison is meaningful since, as found numerically, the transmission coefficient at normal incidence is very sensitive to sample density. An example of the calculated results is shown in Fig. 4, where the experimental data are also indicated. As can be seen in the figure, the agreement between the calculated results based on the measured sample density (i.e., $\rho$ = 2.16 g/cm$^3$) and the experimental data is satisfactory.

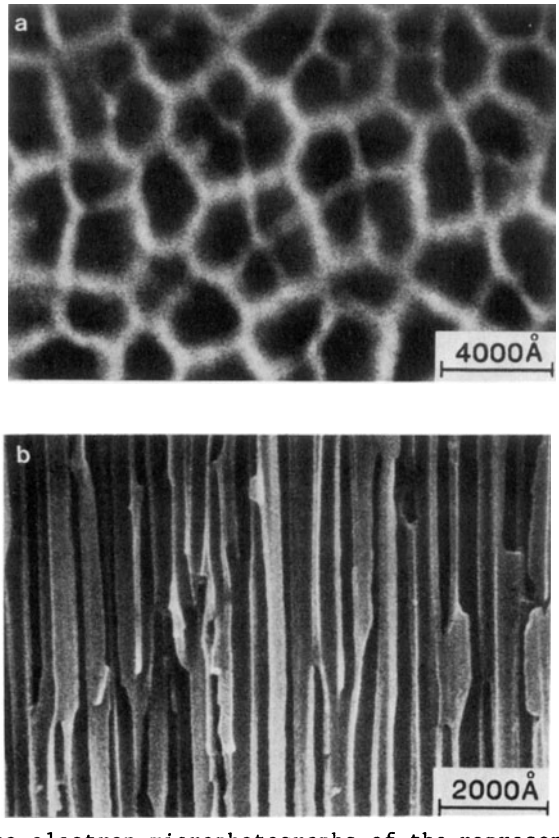


Fig. 3. Scanning electron microphotographs of the representative microstructure of the thin layer anodized $Al_2O_3$. (a) Top surface. (b) Cross section.

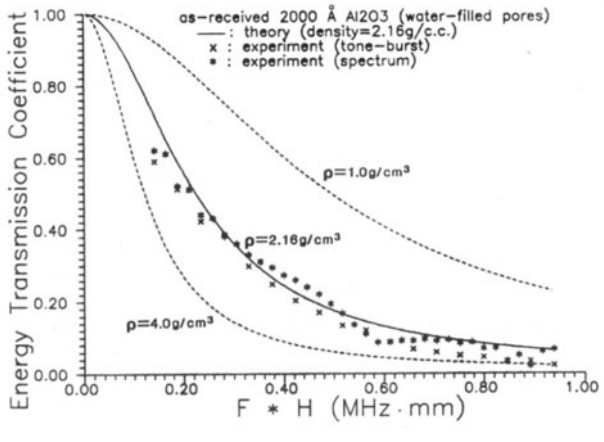


Fig. 4. Normal incident transmission coefficient and its dependence on the sample density. The discrete points are from experiment. The lines are calculated from theory [7] for different sample densities. The theoretical transmission coefficient corresponding to the measured sample density 2.16 g/cm$^3$ is shown as the solid line. The calculated results are in good agreement with the measured data.

## DETERMINATION OF ELASTIC CONSTANTS

Transmission coefficients were measured as a function of incident angle at different frequencies. As an example the measured result at frequency equal 15 MHz (i.e., fh = 0.752 MHz mm) is shown in Fig. 5. To reconstruct the elastic constants from the measurements, we used a non-linear least square technique for best data fitting of minimum- and maximum-transmission angles at different frequencies. The algorithm is to adjust $E_1$ for best data fitting of the minimum-transmission angles. From this we can reconstruct the in-plane Young's modulus $E_1$. Subsequently, using the reconstructed $E_1$ and adjusting $G_{13}$ for best fitting of the maximum-transmission angles, we can obtain the interlayer shear modulus $G_{13}$. A summary of the measured minimum- and maximum-transmission angles at different frequencies and the best-fit data curves are shown in Fig. 6. The reconstructed $E_1$ and $G_{13}$ are given in Table 1. It should be noted that the results of reconstruction do not depend on the selection of the initial values of elastic constants used in the reconstruction.

An example of the calculated transmission coefficient based on the reconstructed elastic constants is shown in Fig. 5. The calculated results and the experimental data are in good agreement. Note that the first maximum is not observed in the experiments. This is a result of the ultrasonic attenuation and finiteness of the beam width.

## THEORETICAL ESTIMATION OF ELASTIC CONSTANTS

Consider the porous $Al_2O_3$ structure as a two-phase composite, where pure $Al_2O_3$ is the primary phase which forms the skeleton and the pores are the second phase which can be air, water, primer or any other substance that fills the pores. Since the pores are vertical through-thickness, the composite can be considered to be transversely isotropic with the symmetry axis in the plate normal direction. For such a composite, a number of models [9,10] are available to calculate the effective elastic constants from the bulk properties of the two constituents. The primary phase $Al_2O_3$ has Young's modulus and Poisson's ratio $E_p$ = 402.0 GPa and $\nu_p$ = 0.2256, and the second phase water (i.e., the pores are filled with water) has $E_s \approx 0$ GPa and $\nu_s$ = 0.5. The effective elastic constants calculated from models are shown in Table 1.

As shown in Table 1, the estimated elastic constants calculated from Nielsen's model are in good agreement with those obtained from the experiment. Further use of Nielsen's model in the estimation of the effective elastic constants of porous aluminum oxide has been adopted.

## CONCLUSION

We have demonstrated that a reconstruction of the in-plane Young's modulus of a thin layer of $Al_2O_3$ can be achieved through the measurement of the angle of minimum transmission coefficient. Subsequent reconstruction of the interlayer shear modulus of the thin layer can be accomplished with measurements of maximum-transmission angles at different frequencies. Such an approach is promising for the evaluation of more general (i.e., less symmetric) anisotropic thin plates.

Based on the experimentally obtained elastic constants in our work, a use of Nielsen's model [9] to estimate the effective elastic constants of a thin layer of anodized $Al_2O_3$ is recommended.

Table 1. THE EFFECTIVE ELASTIC MODULI OF THE THIN LAYER OF ANODIZED $Al_2O_3$

| | $E_1$(GPa) | $G_{12}$(GPa) | $\nu_{12}$ | $E_3$(GPa) | $G_{13}$(GPa) | $\nu_{13}$ |
|---|---|---|---|---|---|---|
| Nielsen | 38.50 | 14.94 | 0.2883 | 156.8 | 24.94 | 0.393 |
| Klyavlin | 72.65 | 28.05 | 0.2946 | 156.8 | | 0.2256 |
| Experiment | 36.7 | | | | 17.4 | |

Subscripts 1 and 2 denote two orthogonal directions in the plane of the plate; subscript 3 represents the plate normal direction.

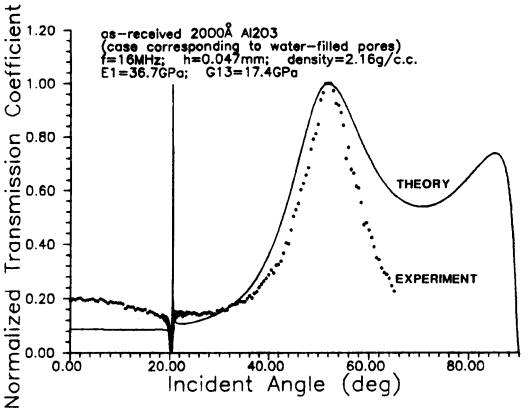


Fig. 5 The measured and calculated transmission coefficients as a function of incident angle. The measured data are shown as discrete points. These data are overlaid on the theoretical transmission coefficients calculated by using the reconstructed elastic constants $E_1$ and $G_{13}$. The other elastic moduli needed for calculation are taken from Nielsen's model (see Table 1).

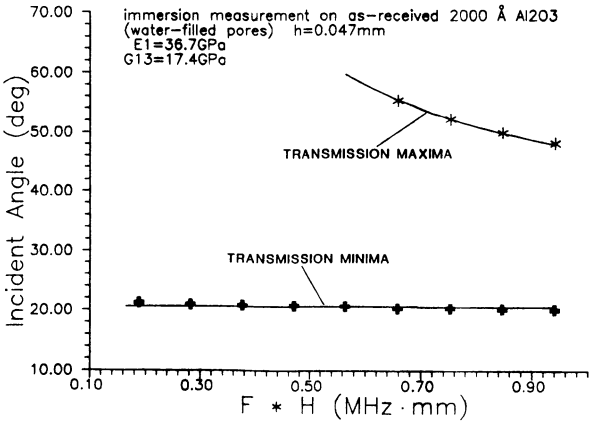


Fig. 6 The minimum- and maximum-transmission angles as functions of the product of frequency and sample thickness. The experimental data are shown as points. The best fitting curves, overlaid with the measured data, are obtained from the optimization of $E_1$ to fit the minimum-transmission angles and subsequently of $G_{13}$ to fit the maximum-transmission angles.

ACKNOWLEDGEMENTS

This work was sponsored by the Center for Advanced NDE, operated by the Ames Laboratory, USDOE, for the Air Force Wright Aeronautical Laboratories/Materials Laboratory under contract #SC-80-148B. The authors also express their appreciation to Prof. Y. J. Wang for his helpful discussion.

REFERENCES

1. G. D. Davis and J. D. Venables, in Durability of Structural Adhesives, A. J. Kinloch ed., Applied Science Publishers, N.Y. 43-84 (1983).
2. J. A. Marceau, in Adhesive Bonding of Aluminum Alloys, E. W. Thrall and R. W. Shannon eds., Marcel Dekker Inc., N.Y., 51-74 (1985).
3. S. I. Rokhlin, Y. J. Wang and W. Wang, this proceeding.
4. A. H. Nayfeh and D. E. Chimenti, J. Appl. Mech., 55, 863-870 (1988).
5. S. I. Rokhlin, C. Y. Wu and L. Wang, this proceeding.
6. D. E. Chimenti and A. H. Nayfeh, J. Appl. Physics, 33, 4531-4538 (1985).
7. F. I. Solyanik, Sov. Phys. Acoust., 23(6), 533-536 (1977).
8. E. L. Shenderov, Sov. Phys. Acoust., 30(1), 69-73 (1984).
9. L. N. Nielsen, Material Sci. and Eng., 52, 39-62 (1982).
10. V. V. Klyavlin, Mechanika Polimerov, 5, 812-817 (1970) (in Russian).